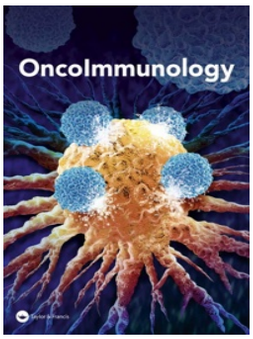

OncoImmunology

ISSN: (Print) (Online) Journal homepage: www.tandfonline.com/journals/koni20

# Smad7 is a negative regulator of immunogenic cell death in colorectal cancer

Claudia Maresca, Eleonora Franzè, Federica Laudisi, Marco Colella, Andrea Iannucci, Rachele Frascatani, Ivan Monteleone, Carmine Stolfi & Giovanni Monteleone

**To cite this article:** Claudia Maresca, Eleonora Franzè, Federica Laudisi, Marco Colella, Andrea Iannucci, Rachele Frascatani, Ivan Monteleone, Carmine Stolfi & Giovanni Monteleone (2025) Smad7 is a negative regulator of immunogenic cell death in colorectal cancer, OncoImmunology, 14:1, 2490346, DOI: 10.1080/2162402X.2025.2490346

**To link to this article:** https://doi.org/10.1080/2162402X.2025.2490346

ONCOIMMUNOLOGY
2025, VOL. 14, NO. 1, 2490346
https://doi.org/10.1080/2162402X.2025.2490346

Taylor & Francis
Taylor & Francis Group

ORIGINAL RESEARCH

OPEN ACCESS Check for updates

# Smad7 is a negative regulator of immunogenic cell death in colorectal cancer

Claudia Maresca[a], Eleonora Franzè[a], Federica Laudisi[a], Marco Colella[a], Andrea Iannucci[b], Rachele Frascatani[a], Ivan Monteleone[b], Carmine Stolfi[a], and Giovanni Monteleone[a,c]

[a]Department of Systems Medicine, University of Rome Tor Vergata, Rome, Italy; [b]Department of Biomedicine and Prevention, University of Rome Tor Vergata, Rome, Italy; [c]Gastroenterology Unit, Policlinico Universitario Tor Vergata, Rome, Italy

**ABSTRACT**

Induction of endoplasmic reticulum (ER) stress is followed by exposure of calreticulin (CRT) on the cancer cell plasma membrane and elicits an anticancer immune response, referred to as immunogenic cell death (ICD). Smad7 is highly expressed by colorectal cancer (CRC) cells, and its knockdown with a specific antisense oligonucleotide (AS) induces ER stress. We hypothesized that, by preventing ER stress, high Smad7 in CRC cells can contribute to limiting ICD. This study aimed to investigate whether targeted inhibition of Smad7 in CRC cells promotes an anti-cancer immune response. Downregulation of Smad7 in the human HCT116 and DLD1 cells and murine CT26 cells promoted calreticulin translocation to the plasma membrane and this phenomenon was prevented by Tauro-urso-deoxycholic acid, an inhibitor of ER stress. Smad7-deficient cells secreted high levels of ATP and HMGB1, thereby promoting the activation of co-cultured dendritic cells. Mice engrafted with Smad7-deficient CT26 cells developed fewer and smaller tumors than wild-type CT26 cell-engrafted mice and exhibited a marked tumor infiltration with $CD8^+$ cells and to a lesser extent $CD4^+$ cells. Depletion of $CD8^+$ T cells abrogated the inhibitory effect of Smad7 knockdown on the tumor volume. Finally, we showed that, in a vaccination model, implanted Smad7-deficient CT26 cells protected mice from the development of tumors induced by wild-type CT26 cells. These data show that Smad7 deficiency triggers ICD in CRC cells, thus reducing tumor development and growth, and suggest that Smad7 inhibitors could be developed as novel ICD inducers, providing a new concept for antitumor immunotherapy.

**ARTICLE HISTORY**
Received 22 October 2024
Revised 2 April 2025
Accepted 3 April 2025

**KEYWORDS**
ATP; calreticulin; cytotoxic T-cells; HMGB1

## Introduction

In colorectal carcinoma (CRC), one of the most frequent cancers in developed countries, the carcinogenetic process follows an established pattern characterized by activation of WNT and RAS signaling, and inhibition of TGF-β function.[1–3] The concerted activity of these pathways generates and maintains a potent CRC cell growth-inducing stimulus.[1] Most of the targeted therapeutics tested to treat metastatic CRC so far have shown little or limited sustained survival benefit.[4] Therefore, a better understanding of the mechanisms responsible for CRC growth and progression may help identify new targets for therapeutic interventions.

Exposure to selected stressors induces in cancer cells endoplasmic reticulum (ER) stress.[5–7] ER stress leads to the translocation of calreticulin (CRT), which is usually contained in the lumen of the endoplasmic reticulum, to the surface of the plasma membrane (ecto-CRT), where it binds to CD91 on the surface of dendritic cells (DCs) and functions as an 'eat me' signal, to facilitate the uptake of tumor-associated antigens by DCs.[7,8] DCs then cross-present tumor antigens to naïve T cells and hence initiate an adaptive anticancer immune response, referred to as "immunogenic cell death" (ICD).[9,10] ICD is preceded by another major premortem phenomenon, namely autophagy, which favors the lysosomal secretion of ATP in the extracellular space, thus promoting the recruitment of DC into the tumor bed.[5,9,11] Radiotherapy and chemotherapeutic agents, such as oxaliplatin and 5-fluorouracil, two compounds used to treat advanced CRC, are capable of inducing ER stress, exposure of CRT on the CRC cell plasma membrane, and eliciting an anticancer immune response.[12–14] Unfortunately, however, residual cancer cells can activate survival signals thus becoming unresponsive to such treatments. The use of additional ICD inducers, as either a supplement or alternative to an existing anti-cancer therapeutic approach, could facilitate the immune-mediated clearance of minimal residual disease and reduce the risk of relapse.[12,15]

We have previously shown that Smad7, an intracellular protein that has been traditionally considered as an inhibitor of Transforming Growth Factor (TGF)-β1, is over-expressed by human CRC and controls positively CRC cell growth, survival, and migration in a TGF-β1-independent manner.[16,17] Further work aimed at dissecting the basic mechanisms by which Smad7 controls CRC cell behavior showed that reduction of Smad7 expression in CRC cells with a specific Smad7 antisense oligonucleotide (AS) upregulates the phosphorylation of eukaryotic translation initiation factor 2α (eIF2α), a phenomenon that is indicative of ER stress.[18–20] Altogether, these observations suggest that, by preventing ER stress, high

**CONTACT** Giovanni Monteleone Gi.Monteleone@Med.uniroma2.it; Carmine Stolfi carmine.stolfi@uniroma2.it Department of Systems Medicine, University of Rome Tor Vergata, Via Montpellier, 1, Rome 00133, Italy

Supplemental data for this article can be accessed online at https://doi.org/10.1080/2162402X.2025.2490346

Smad7 in CRC cells can contribute to limiting immunogenic cell death.

The present study aimed to assess whether targeted inhibition of Smad7 in CRC cells can promote an anti-cancer immune response.

## Materials and methods

### Cell cultures

All reagents were obtained from Sigma-Aldrich (Milan, Italy) unless otherwise specified. DLD1, HCT-116, and CT26 cells were purchased from the American Type Culture Collection (ATCC, Manassas, VA) and TS/A cells. Cells were maintained in RPMI 1640 (DLD1 and CT26), McCoy's 5A (HCT-116), or Dulbecco's modified Eagle's high glucose medium (TS/A) supplemented with 10% fetal bovine serum (FBS; Lonza, Verviers, Belgium) and 1% Penicillin/Streptomycin (P/S) at 37°C, 5% CO2. All cells were used at a passage number between 10 and 25 and were regularly checked for mycoplasma contamination. Cells were transfected with Smad7 sense or AS (0.5–2 μg/ml, GeneLink, Orlando, Florida) as previously described[21] or with a cadherin-11 sense or AS (2 μg/ml, AS-300600, Exiqon, Woburn) for 36 hours. In parallel experiments, cells transfected with Smad7 AS (2 μg/ml) were treated with Tauro-ursodeoxycholic acid (TUDCA, 50 μM). To evaluate whether suppression of Smad7 induced apoptosis, necroptosis, or ferroptosis, DLD1 cells were transfected with Smad7 sense or AS for 48 hours. Staurosporin was used as a positive inducer of apoptosis, a combination of TNF-α (#210-TA, R&D Systems, Minneapolis, MN), Z-VAD-FMK and SM-164 (#HY-16658B and #HY-15989 respectively, both from Med Chem Express, Monmouth Junction, NJ) was used as a positive inducer of necroptosis, erastin (#S7242, Selleckchem, Cologne, Germany) was used as a positive inducer of ferroptosis. To investigate the effect of the pan-caspase inhibitor Q-VD-OPh on CRT exposure on the cell surface, DLD1 cells were pre-treated with Q-VD-OPh (10 μM, #SML0063, R&D Systems) or DMSO (vehicle) for 1 hour and then transfected with Smad7 sense or AS for 36 hours.

### Monocyte-derived dendritic cell activation and phagocytosis

Peripheral blood mononuclear cells were isolated by Ficoll-Hypaque density gradient centrifugation of blood samples obtained from healthy donors and used to purify monocytes using the $CD14^+$ monocyte isolation kit (#130-050-201, Miltenyi Biotec, Bergisch Gladbach, Germany). Monocytes were cultured in a complete medium (RPMI-1640, 10% FBS, 1% P/S) supplemented with recombinant human GM-CSF (50 ng/ml, #130-095-372, Miltenyi Biotec) and recombinant human-IL-4 (250 ng/ml, #130-093-917, Miltenyi Biotec) for 6 days. On day 3, the cytokine-supplemented medium was refreshed. After 6 days, monocyte-derived dendritic cells (MoDCs) were collected and co-cultured with HCT-116 or DLD1 cells (ratio 1:1), which were previously stained with Cell Trace (#C34557, Thermo Fisher Scientific, Waltham, MA) for 30 minutes at 37°C and transfected with Smad7 sense or AS. At the end, cells were recovered, stained with the antibody anti-human CD11c-PerCP/Cy5.5 (#337210, BioLegend, San Diego, CA), anti-human CD86-FITC (#555657, BD Biosciences, San Diego, CA) and anti-human HLA-DRII-PE (#555812, BD Biosciences), and analyzed by Gallios flow cytometer (Beckman Coulter, Milan, Italy).

### Western blotting

Total proteins were extracted on ice using the following lysis buffer: 10 mm HEPES (pH 7.9), 0.1 mm EDTA, 0.2 mm ethylene glycol-bis (β-aminoethyl ether)-N,N,N',N'-tetraacetic acid, 0.5% Nonidet P40 and 10 mm potassium chloride, supplemented with 10 mg/ml aprotinin, 10 mg/ml leupeptin, 1 mm dithiothreitol, 1 mm phenylmethylsulphonyl fluoride, 1 mm sodium vanadate, and 1 mm sodium fluoride. The lysates were separated on an SDS-PAGE gel and transferred using a Trans-Blot Turbo apparatus (Bio-Rad Laboratories, Hercules, CA). Membranes were then incubated with the antibodies anti-human/mouse Smad7 (1:1000, #MAB2029, R&D Systems), anti-human/mouse CRT (1:1000, # PA3–900, Thermo Fisher Scientific), anti-human cleaved caspase-3 (1:1000, #9661S, Cell Signaling Technology, Danvers, MA), anti-human HMGB1 (1:1000, #39355, Cell Signaling), anti-human GPX4 (1:1000, #HY-P80692, Med Chem Express), anti-human p-MLKL Ser358 (1:1000, #91689S, Cell Signaling Technology), anti-human p-RIP3 Ser227 (1:1000, #EPR9627, Abcam, Cambridge, UK), or anti-human/mouse β-actin (1:5000) and, subsequently, with a secondary antibody conjugated to HRP (1:20000, Dako, Santa Clara, CA). Membrane imaging was done using chemiluminescence with the ChemiDoc Imaging System (Bio-Rad Laboratories).

### Ecto-calreticulin analysis

At the end of each experiment, cells were washed with 1× PBS (supplemented with 5% FBS and 0.1% sodium azide) and fixed with 0.25% formaldehyde for 5 minutes. Afterward, cells were washed and incubated with an antibody against CRT (1:100, # PA3–900, Thermo Fisher Scientific) for 30 minutes. Cells were then washed and incubated with a FITC-conjugated secondary antibody (1:500, #ab6717, Abcam) and 7-AAD (1:500, #51-68981E, BD Biosciences). In parallel, cells were stained with a control isotype primary antibody. Ecto-CRT expression in live cells (7-AAD-negative cells) was evaluated by flow cytometry. In addition, DLD1 cells were labeled for CRT and PE-conjugated Annexin V (1:500, #51-65875X, BD Biosciences) and the percent of cells expressing Annexin V and/or ecto-CRT was evaluated by flow cytometry.

### Assessment of cell death

DLD1, HCT-116 and CT26 cells were transfected with Smad7 sense or AS for 48–60 hours. In addition, DLD1 cells were pre-treated with Q-VD-OPh (10 μM) or DMSO (vehicle) for 1 hour and then transfected with Smad7 sense or AS for 60 hours. Cells were then collected, stained with FITC-Annexin V (1:100, #31490013, Immunotools, Friesoythe, Germany) according to the manufacturer's instructions, and incubated with

propidium iodide (PI) (5 µg/ml) for 30 min at 4°C. Cell death was quantified using Gallios flow cytometer.

### ATP and HMGB1 quantification assays

Cell-free supernatants of CRC cell lines transfected with Smad7 sense or AS were used to quantify extracellular ATP by the luciferase/luciferin-based ENLITEN ATP Assay (#FF2000, Promega, Madison, WI). Intracellular and extracellular HMGB1 were evaluated in total extracts and cell-free supernatants, both derived from CRC cell lines transfected with Smad7 sense or AS for 48–60 hours, by Western blotting and enzyme-linked immunosorbent assay (#30164033, IBL International GmbH, Hamburg, Germany), respectively.

### Real-time PCR

Total RNA was extracted from CRC cells transfected with Smad7 sense or AS using PureLink mRNA mini-kit (#12183025, Thermo Fisher Scientific). A constant amount of RNA (1 µg/sample) was retrotranscribed into complementary DNA (cDNA). Reverse transcription was performed with Oligo(dT) primers and with M-MLV-reverse transcriptase (#28025021, Thermo Fisher Scientific). The cDNA was then amplified by real-time PCR using iQ SYBR Green Supermix (Bio-Rad Laboratories). Primers were as follows: human CRT: Fwd 5′- TGATCCCACAGACTCCAAGC-3′, Rev 5′-CGTCCATCTCTTCATCCCAG-3′; human β-actin: Fwd 5′-AAGATGACCCAGATCATGTTTGAGACC-3′, Rev 5′-AGCCAGTCCAGACGCAGGAT-3′. RNA expression was calculated relative to the housekeeping β-actin gene using the ΔΔCt algorithm.

### Animal tumor models

Immunocompetent, 6-week-old female BALB/c mice (Charles River Laboratories, Lodi, Italy) were maintained in cages with filter tops and provided with sterilized food and water at the animal facility of the University of Rome 'Tor Vergata' (Rome, Italy). All animal experiments received approval from the local Institutional Animal Care and Use Committee (authorization 794/2023-PR) and were registered with the Italian Ministry of Health.

CT26 cells transfected with Smad7 AS (2 µg/ml) or sense oligonucleotides for 48 hours were subcutaneously implanted into the left flank of immunocompetent BALB/c mice ($7 \times 10^5$ per mouse in 100 µl PBS) whose fur was previously shaved (day 0). Tumor growth was monitored until the time of sacrifice (day 14). Tumor-infiltrating leukocytes (TILs) were isolated through enzymatic digestion using Liberase TM (200 µg/ml, #05401127001) and DNase I (200 µg/ml, #11284932001) (both from Roche Diagnostics GmbH, Mannheim, Germany). To deplete $CD8^+$ cells in vivo, mice were intraperitoneally injected with an anti-mouse CD8 antibody (100 µg per mouse; #100764, Biolegend) starting two days before CT26 injection and continuing every four days until day 10. $CD8^+$ cell depletion was assessed in murine splenocytes by flow cytometry.

In the tumor vaccination assay, CT26 cells were transfected with Smad7 AS (2 µg/ml) or treated with Mitomycin C for 48 hours. Cells were then subcutaneously implanted into the left flank of immunocompetent BALB/c mice ($7 \times 10^5$ per mouse in 100 µl PBS) whose fur was previously shaved (day −7). After one week (day 0), mice were re-challenged with live CT26 cells or TS/A cells ($7 \times 10^5$ per mouse in 100 µl PBS) into the right flank. Tumor growth was monitored until the time of sacrifice (day 14).

### Flow cytometry

Tumor infiltrating leukocytes isolated from CT26-derived tumors were stimulated with phorbol myristate acetate (10 ng/ml), ionomycin (1 µg/ml), and brefeldin A (10 µg/ml; #00-4506-51, Thermo Fisher Scientific) for 4 hours. Cells were then collected and stained with live/dead cell assay (#L34966A, Thermo Fisher Scientific) and the following antibodies: anti-mouse CD45-APC-H7 (#557659), CD3-Pacific Blue (#558214), CD8-PerCP-Cy5.5 (#551162), DX5-PE (#553858) (1:50 final dilution, BD Biosciences), or the corresponding isotype control antibodies. The fluorescence signals were then analyzed using Gallios flow cytometer and Kaluza software (Beckman Coulter).

### Immunofluorescence

Tumor cryosections were fixed using 4% paraformaldehyde for 10 minutes. Sections were then washed with PBS 1X and permeabilized with 0.1% Triton-X for 10 minutes. Blocking procedure (BSA 1%, Tween 0.1%, Glycine 2%) was performed for 1 hour at room temperature and the slides were incubated with a rat primary antibody anti-mouse CD4 (1:100, #550278, BD Biosciences) or rabbit primary antibody anti-mouse CD8 (1:100, #AB251609, Abcam) overnight at 4°C. After washing with PBS 1X, slides were incubated with a secondary antibody goat anti-Rat Alexa488 (1:2000, #A11006, Thermo Fisher Scientific) or goat anti-rabbit Alexa 568 (1:2000, #A11011, Thermo Fisher Scientific) for 2 hours at room temperature. Slides were then washed, mounted using Prolong gold antifade reagent with DAPI (#P36931, Thermo Fisher Scientific) and analyzed by LEICA DMI4000 B microscope using the LEICA application suite software (V4.6.2) (Leica, Wetzlar, Germany).

### Statistical analysis

Parametric data were analyzed using the two-tailed Student's t-test for comparison between two groups or one-way analysis of variance (ANOVA) for multiple comparisons. GraphPad Prism 9 (GraphPad Software, La Jolla, CA) was used for statistical and graphical data evaluations. $p$ values $< 0.05$ were considered statistically significant.

## Results

### Smad7 knockdown in CRC cells is accompanied by hallmarks of immunogenic cell death

The induction of ER stress is accompanied by enhanced translocation of CRT on the cancer cell surface.[5] Because our

previous work showed that Smad7 protein inhibition induces ER stress,[18–20] we evaluated whether Smad7 down-regulation increased the exposure of CRT on the CRC cell surface. Flow cytometry analysis showed that transfection of DLD1 and HCT-116 with Smad7 AS for 36 and 24 hours respectively dose-dependently increased the percentage of ecto-CRT-expressing live cells as compared to control (sense-treated) cells (Figure 1A, Suppl. Fig. S1 and Suppl. Fig. S2A). At the same time point, Smad7 AS enhanced the fraction of cell death but this was evident only at the highest concentration (i.e. 2 µg/ml) (Suppl. Fig. S1 and Suppl Fig. S2B). Gating on viable cells confirmed ecto-CRT induction following Smad7 down-regulation (Suppl. Fig.S1). In contrast, no change in the percentage of ecto-CRT-expressing DLD1 cells was seen following transfection with a specific cadherin 11 AS (Suppl. Fig. S3).

To evaluate whether, in Smad7-deficient cells, the increase in ecto-CRT was secondary to its translocation from the ER to the cell membrane rather than to the upregulation of CRT expression, we analyzed CRT mRNA and total CRT protein in the cultured cells. Smad7 protein reduction did not alter the total amount of CRT protein (Figure 1B) and RNA (Figure 1C). Treatment of DLD1 cells with TUDCA, an inhibitor of ER stress, prevented the Smad7 AS-driven CRT translocation on the CRC cell surface (Figure 1D).

Double-labeling for CRT and Annexin V showed that Smad7 AS enhanced the fractions of cells co-expressing ecto-CRT and Annexin V (Figure 2A), as well as cleavage of caspase-3 (Figure 2B) thus suggesting a link between apoptosis and induction of ICD. Consistently, treatment of cells with Q-VD-OPh, a pan-caspase inhibitor, reverted the induction of cell death and ecto-CRT seen following Smad7 inhibition (Figure 2C–D). As other cell death mechanisms, such as necroptosis and ferroptosis, are also immunogenic,[22] we investigated whether Smad7 suppression leads to the induction of

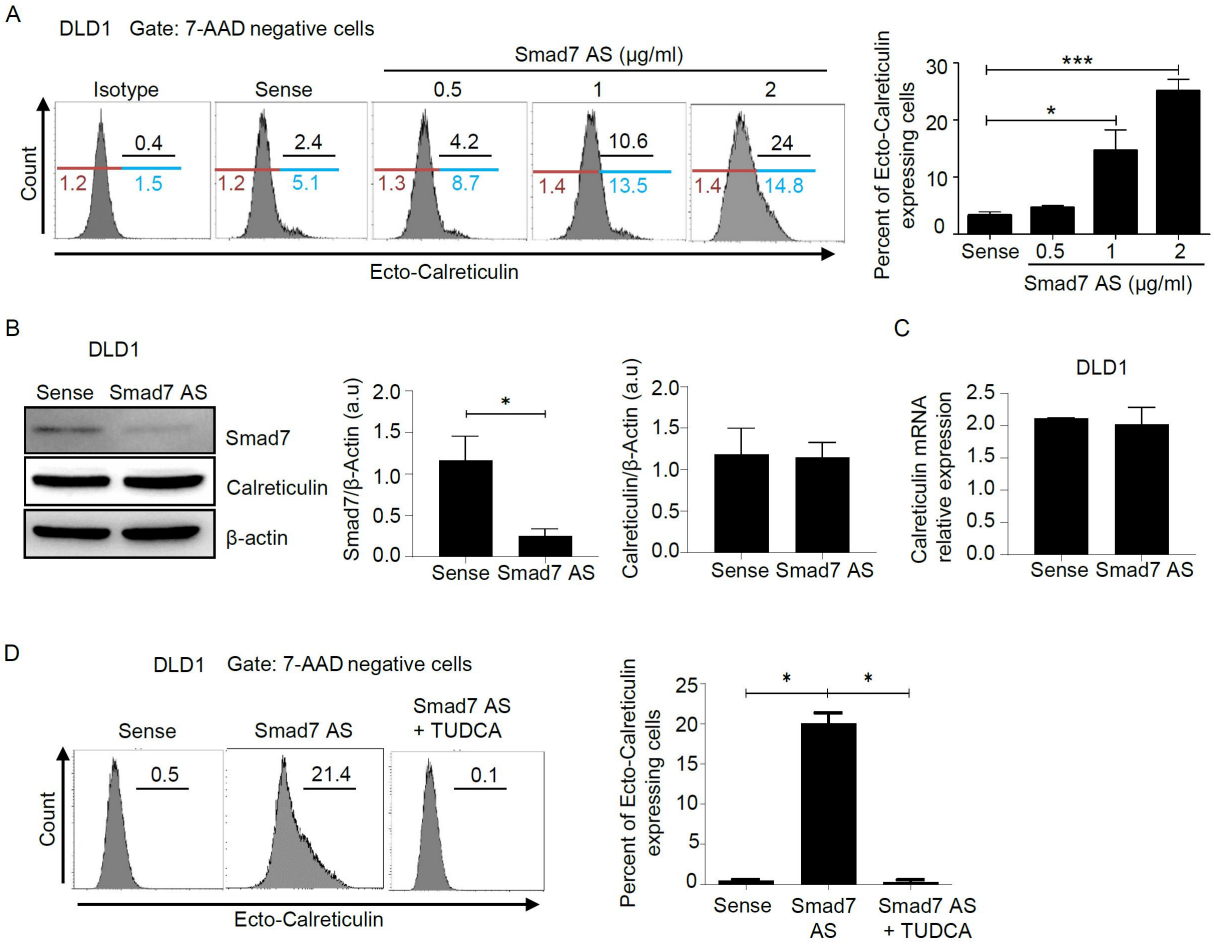


**Figure 1.** Downregulation of Smad7 protein expression enhances calreticulin exposure on the cancer cell surface (ecto-calreticulin). (A) Representative histograms showing the percentage of ecto-calreticulin-expressing DLD1 cells as assessed by flow cytometry. Cells were transfected with either Smad7 as or sense for 36 hours. Mean fluorescence intensity (MFI) values for calreticulin staining in both ecto-calreticulin-negative cells (red bars) and ecto-calreticulin-positive cells (blue bars) are also indicated. Staining with an isotype control antibody for calreticulin is also shown. Right inset: histograms showing the percentage of ecto-calreticulin-expressing DLD1 cells transfected with either Smad7 as or sense for 36 hours. Data are mean ± SD of six separate experiments. Data were analyzed using one-way analysis of variance (ANOVA) followed by Dunnett's post hoc test. *$p < 0.05$; ***$p < 0.001$. (B) Representative western blots for Smad7, calreticulin, and β-actin in total extracts of DLD1 cells transfected with Smad7 as or sense for 24 hours. β-actin was used as a loading control. The right panels show the mean ± SEM of all experiments; the differences were evaluated using a two-tailed Student's t-test. * $p < 0.05$. (C) DLD1 cells were either transfected with Smad7 as or sense for 24 hours. Calreticulin RNA transcripts were evaluated by the real-time polymerase chain reaction. Levels were normalized to β-actin. Values indicate the mean ± SD of three separate experiments. Differences were analyzed using a two-tailed Student's t-test. (D) DLD1 cells were pre-treated or not with TUDCA (50 µM) and then transfected with Smad7 as or sense (both used at 2 µg/ml) for 36 hours. Representative histograms showing the percentage of ecto-calreticulin-expressing DLD1 cells. Results indicate the percentage of ecto-calreticulin-expressing cells as assessed by flow cytometry. Right inset: data indicate mean ± SD of all experiments. Data were analyzed using one-way analysis of variance (ANOVA) followed by Dunnett's post hoc test. *$p < 0.05$.

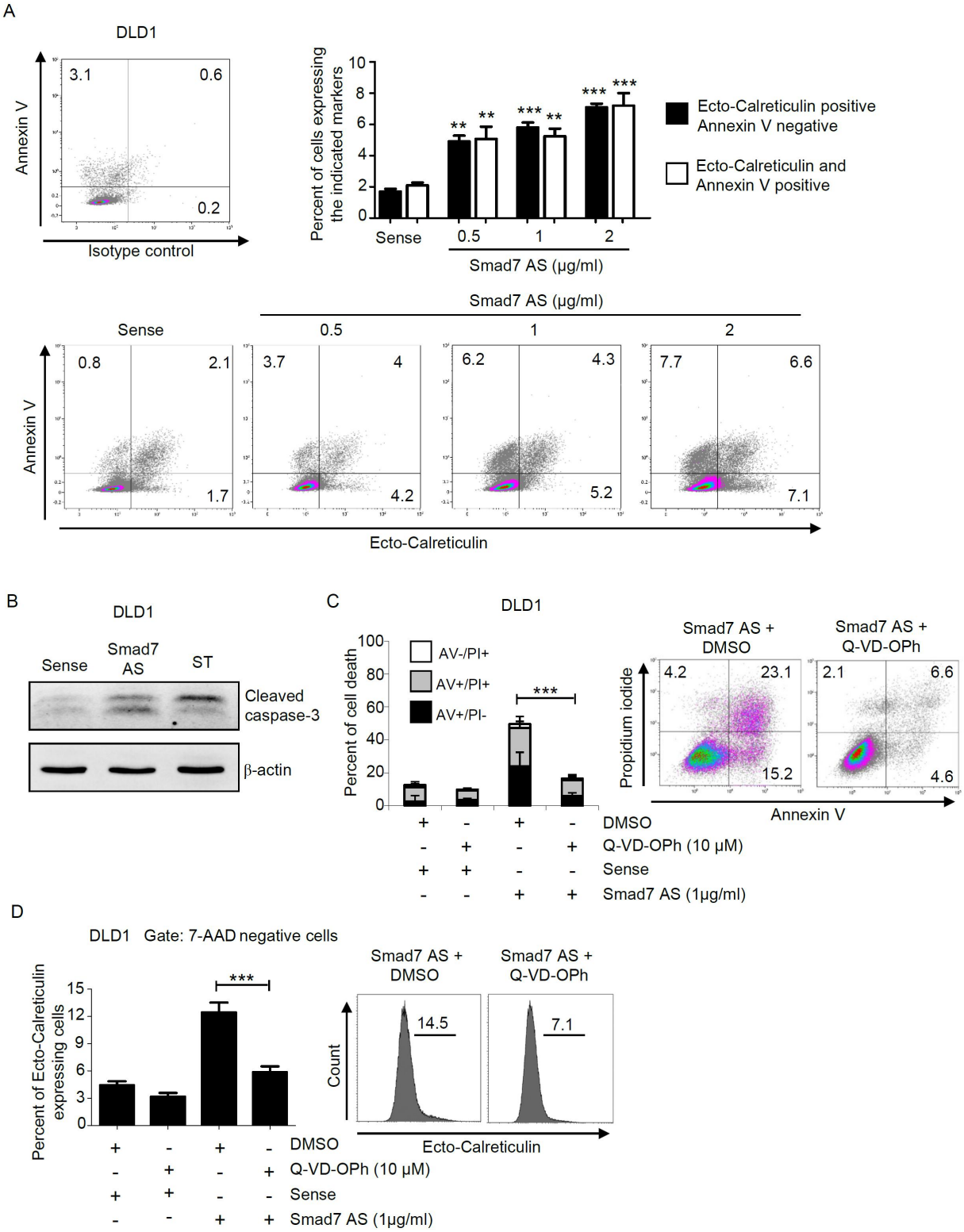


**Figure 2.** Involvement of apoptotic cell death in the Smad7 suppression-driven induction of ecto-calreticulin (A) Representative density plots showing the percentage of DLD1 cells expressing calreticulin exposed on the cell surface (ecto-calreticulin) and Annexin V. Cells were transfected with either Smad7 as or sense for 36 hours. Results indicate the percentage of annexin V and/or ecto-calreticulin expressing cells as assessed by flow cytometry. Staining with an isotype control antibody for calreticulin is also shown. Upper right inset: histograms showing the percentage of annexin V and/or ecto-calreticulin expressing DLD1 cells transfected with either Smad7 as or sense for 36 hours. Data are mean ± SD of three separate experiments. Data were analyzed using one-way analysis of variance (ANOVA) followed by Tukey's post hoc test. Smad7 as-transfected cells vs sense-transfected cells: $^{**}p < 0.01$; $^{***}p < 0.001$. (B) Representative Western blots for cleaved caspase-3 and β-actin in total extracts of DLD1 cells transfected with Smad7 sense or as for 48 hours. Protein lysates derived from DLD1 cells treated with 1 μg/ml staurosporin for 18 hours (ST) were used as a positive control of caspase 3 cleavage. β-actin was used as a loading control. (C) Histograms showing the percentage of cell death in DLD1 cells pre-treated with either Q-VD-OPh or DMSO (vehicle) for 1 hour and then transfected with Smad7 sense or as for 60 hours. Data indicate mean ± SD of three separate experiments. Annexin V (AV) and/or propidium iodide (pi)-positive cells were evaluated by flow cytometry. Data were analyzed using one-way analysis of variance (ANOVA) followed by Dunnett's post hoc test. $^{***}p < 0.001$. Right inset: Representative density plots showing the percentages of AV- and/or pi-positive cells treated as indicated. (D) Histograms showing the percentage of ecto-calreticulin expressing DLD1 cells. Cells were pre-treated with either Q-VD-OPh or DMSO (vehicle) for 1 hour and then transfected with Smad7 sense or as for 36 hours. Data indicate mean ± SD of three separate experiments. Data were analyzed using one-way analysis of variance (ANOVA) followed by Dunnett's post hoc test. $^{***}p < 0.001$. Right inset: representative histograms showing the percentage of ecto-calreticulin-expressing DLD1 cells treated as indicated as assessed by flow cytometry.

necroptosis and/or ferroptosis. However, our findings do not support a significant involvement of these pathways of cell death in Smad7 suppression-driven ICD. (Suppl. Fig. S4 A-B).

To evaluate whether Smad7-deficient cells exhibit other markers of ICD, we measured the extracellular levels of ATP, an endogenous adjuvant signal secreted by dying neoplastic cells and able to stimulate recruitment of DCs into the tumor bed and facilitate DC.[5,9] Smad7 protein reduction enhanced the extracellular levels of ATP (Figure 3A and Suppl. Fig. S5A), as well as the release in the culture supernatants of HMGB1 (Figure 3B and Suppl. Fig. S5B), a nonhistone chromatin-binding protein, the binding of which to DC receptors is essential for activating DCs.[5,9] Consistently, analysis of total cellular HMGB1 showed that Smad7 protein downregulation decreased the intracellular content of HMGB1 (Figure 3C). Time-course studies showed that ecto-CRT expression was maximally induced at 36 hours in DLD-1 and at 24 hours in HCT-116 following treatment with 1 μg/ml Smad7 AS as compared to control cells (Suppl. Fig. S6). The reduction of Smad7 protein expression was accompanied by enhanced secretion of ATP at 48 and 36 hours in DLD1 and HCT-116 cells respectively (Suppl. Fig S6). Finally, HMGB1 secretion was evident

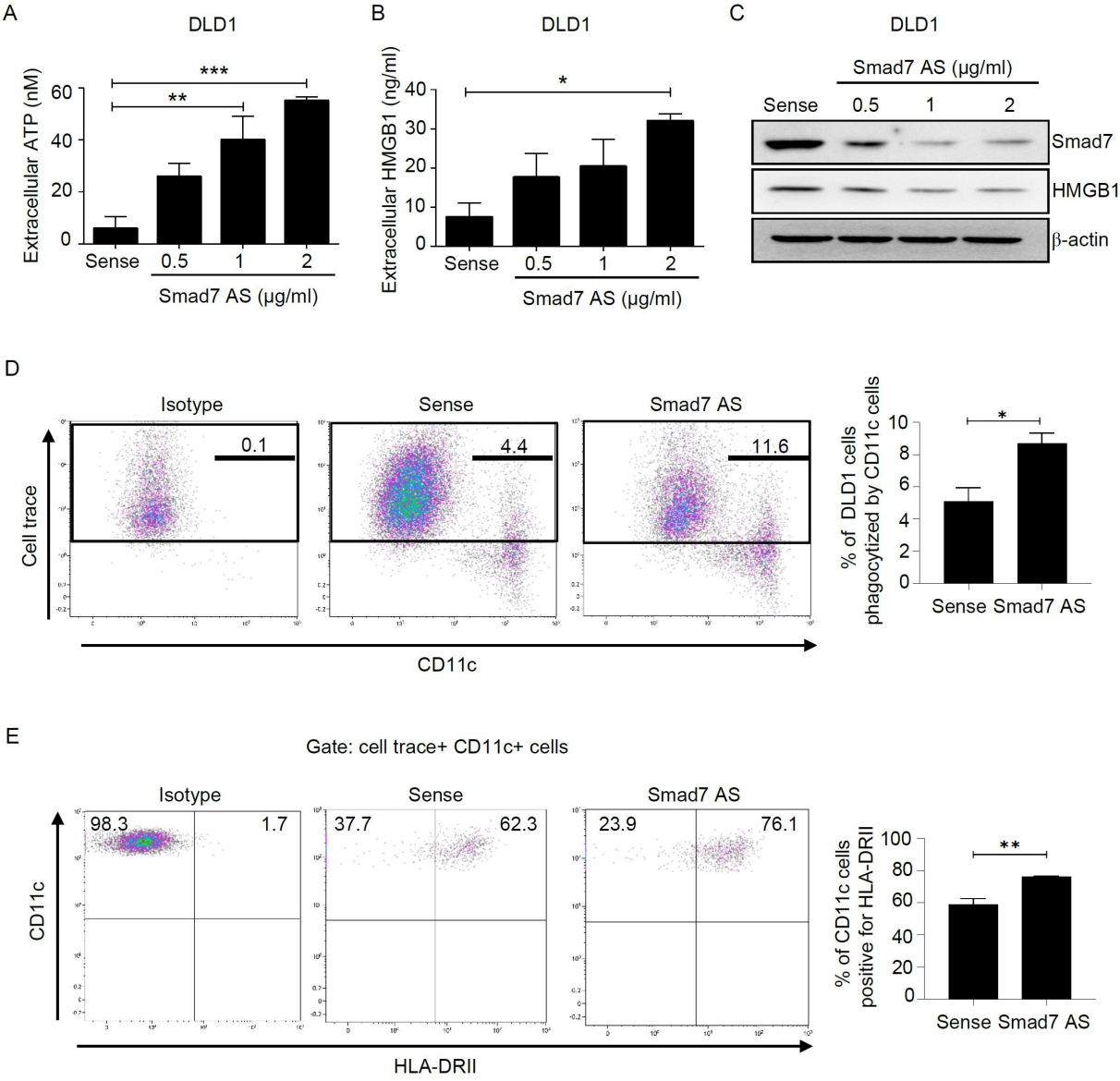


**Figure 3.** Downregulation of Smad7 protein expression in DLD1 cells enhances the secretion of ATP and HMGB1 and the activation of co-cultured dendritic cells. (A) Histograms showing the concentrations of ATP secreted in the culture medium of DLD1 cells transfected with Smad7 as or sense for 48 hours and measured by a luciferase assay. Data are expressed as mean ± SD of all experiments. Data were analyzed using one-way analysis of variance (ANOVA) followed by Dunnett's post hoc test. $^{**}p < 0.01$, $^{***}p < 0.001$. (B) Histograms showing the concentration of HMGB1 secreted in the culture medium of DLD1 cells transfected with Smad7 as or sense for 60 hours and measured by ELISA. Data are expressed as mean ± SD of all experiments. Data were analyzed using one-way analysis of variance (ANOVA) followed by Dunnett's post hoc test. $^{*}p < 0.05$. (C) Representative western blots for Smad7, HMGB1, and β-actin in DLD1 cells transfected with either Smad7 as or sense. β-actin was used as a loading control. (D) Representative density plots showing the percentage of $CD11c^{+}$ that have phagocytized cell-trace labeled DLD1 cells transfected with Smad7 as or sense. Staining with an isotype control antibody for CD11c is also shown. The right panel indicates the mean ± SD of all experiments. Data were analyzed using a two-tailed Student's t-test. $^{*}p < 0.05$. (E) Representative density plots showing the percentage of $HLA\text{-}DRII^{+}$ cells gated as indicated. Staining with an isotype control antibody for HLA-DRII is also shown. The right panel indicates the mean ± SD of all experiments. Data were analyzed using a two-tailed Student's t-test. $^{**}p < 0.01$.

only at 60 and 48 hours in DLD1 and HCT-116 cells respectively, consistent with the induction of cell death at these later time points (Suppl. Fig S6).

Since efficient engulfment of dying cancer cells by DCs and by tissue macrophages is interrelated with the antitumor response,[8] we analyzed if Smad7-deficient cells could be swallowed up by in vitro differentiated human blood monocyte-derived DCs. For this purpose, CRC cells were labeled with the cell trace-violet dye, and phagocytosis was assessed by co-culturing these cells with DCs. Flow cytometry showed that the co-culture of DCs with Smad7-deficient cells enhanced significantly the percentage of $CD11c^+$ DCs engulfing CRC cells as well as the fraction of $CD11c^+$ DCs expressing HLA-DRII (Figure 3D–E and Suppl. Fig. S5C-D).

Taken together, these results suggest that Smad7 knockdown could promote ICD in CRC cells.

### *Smad7 sustains the in vivo CRC growth*

To examine whether cancer cell-derived Smad7 controls the in vivo anti-cancer immune response, we compared the growth of tumors induced by grafting BALB/c mice with the murine CT26 cells transfected either with control or Smad7 AS. In initial experiments, we confirmed that, in line with the human data, CT26 cells transfected with graded doses of Smad7 AS exhibited a dose-dependent induction of ecto-CTR and enhanced release of ATP and HMGB1, while induction of cell death at 36 hours occurred only after transfection with the highest dose of Smad7 AS (Suppl. Fig S7A-E). Time-course studies revealed that Smad7 AS-transfected CT26 cells exhibited a time-dependent induction of cell death with nearly 60% of cell death seen at 48 hours (Suppl. Fig. S7F). Therefore, we selected this time point for the subsequent in vivo studies.[23]

On day 14, the tumors were excised and photographed, and their volume was calculated. CT26-derived tumors knocked out for Smad7 grew significantly less than tumors expressing endogenous Smad7 (Figure 4A–B). Flow cytometry analysis of the tumor-infiltrating CD45-positive cells showed that the microenvironment of Smad7-knocked CT26-derived tumors had higher fractions of both $CD3^+CD8^+$ T cells and $CD3^+CD8^-$ T cells (Figure 4C and Suppl. Fig. S8A), while the fractions of $DX5^+$ cells were not significantly changed by Smad7 knockdown (Suppl. Fig. S8A-B). These data were confirmed by immunofluorescence staining of tumor sections, which showed that tumors developed from Smad7-deficient CT26 cells contained more $CD8^+$ cells and to a lesser extent $CD4^+$ cells than those developed from Smad7-containing CT26 cells (Figure 4D–E).

To evaluate whether the reduced tumor growth in mice engrafted with Smad7-deficient CT26 cells was dependent on cytotoxic $CD8^+$ T cells, Smad7-deficient CT26 cells were implanted in wild-type BALB/c treated with a control or $CD8^+$ T depleting antibody (Suppl. Fig. S9A). Flow-cytometry analysis of splenic $CD45^+$ cells showed that injection of anti-CD8 antibody depleted $CD8^+$ T cells (Suppl. Fig. S9B). Notably, the depletion of $CD8^+$ T cells abrogated the inhibitory effect of Smad7 deficiency on the tumor volume (Figure 4F).

These data indicate that the downregulation of Smad7 protein expression is sufficient to trigger a $CD8^+$ T cell-dependent immune response that restrains the *in vivo* growth of CRC cells.

### *Smad7 knockdown in cancer cells induces immunogenic cell death*

Having shown that a decrease of Smad7 expression in CRC cells is followed by markers of ICD and stimulates *in vivo* the function of cytotoxic $CD8^+$ T cells, we explored the possibility that mice engrafted with Smad7-deficient CT26 cells may exhibit an activated ICD. The gold standard criterion of ICD is protection from secondary tumor challenges after vaccination with tumor cells undergoing ICD.[23] For this purpose, mice were vaccinated with either mitomycin C-treated CT26 cells or Smad7-knocked CT26 cells subcutaneously injected in the left flank and challenged on the right flank one week later with wild-type CT26 cells (Suppl. Fig S9C). Following re-challenge with wild-type CT26 cells, tumors developed in 15/15 mice vaccinated with mitomycin C-treated cells and 3 out of 15 mice vaccinated with Smad7-knocked cells (Figure 5A–C). To ascertain whether the Smad7 knocked-CT26 cell-mediated tumor vaccination effects were specific, we compared the effect of Smad7 AS-transfected cells on tumors induced by injection of either CT26 or TS/A cells (Suppl. Fig. S9D), a murine mammary adenocarcinoma cell line that expresses a repertoire of antigens different from those of CT26 cells. To this end, two groups of mice were vaccinated with CT26 cells transfected with Smad7 AS for 48 hours. One week later, one group of mice was challenged with wild-type CT26 cells and the other one with TS/A cells. At the site of vaccination, there was no difference in terms of tumor volume between the two groups of mice receiving Smad7-deficient CT26 cells and subsequently injected with either CT26 or TS/A cells. The vaccination of mice with Smad7-deficient CT26 cells prevented the development of tumors induced by a secondary challenge with CT26 cells but not that of tumors induced by injection of TS/A cells (Figure 5D).

Overall, these data indicate that Smad7-deficient CT26 cells induce in vivo a specific anti-cancer immunity.

## Discussion

This study was a follow-up of our previous work showing that Smad7 is up-regulated in human sporadic CRC cells and downregulation of Smad7 protein content in CRC cell lines is followed by an arrest of the cell cycle, and eventually apoptosis.[24] Analysis of molecular events underlying the effect of Smad7 deficiency on CRC cell behavior showed that reduction of Smad7 protein expression in CRC cells was accompanied by enhanced phosphorylation of eIF2 α and induction of Activating Transcription Factor (ATF) 4 and CCAAT/enhancer binding protein Homology Protein (CHOP), two downstream targets of eIF2α.[18] Among the upstream kinases that control eIF2α phosphorylation, only the serine-threonine Protein Kinase RNA (PKR) was activated by Smad7 AS, and silencing of PKR inhibited the Smad7 AS-induced eIF2α phosphorylation and ATF4/CHOP induction.[18] Tumor-specific immune responses induced by several therapeutics (e.g. anthracyclines and oxaliplatin) are supposed to rely on ICD, and ER stress response occurs in all scenarios of ICD.[5,12] In the present study, in vitro and in vivo experiments were performed to investigate whether Smad7 knockdown increases the

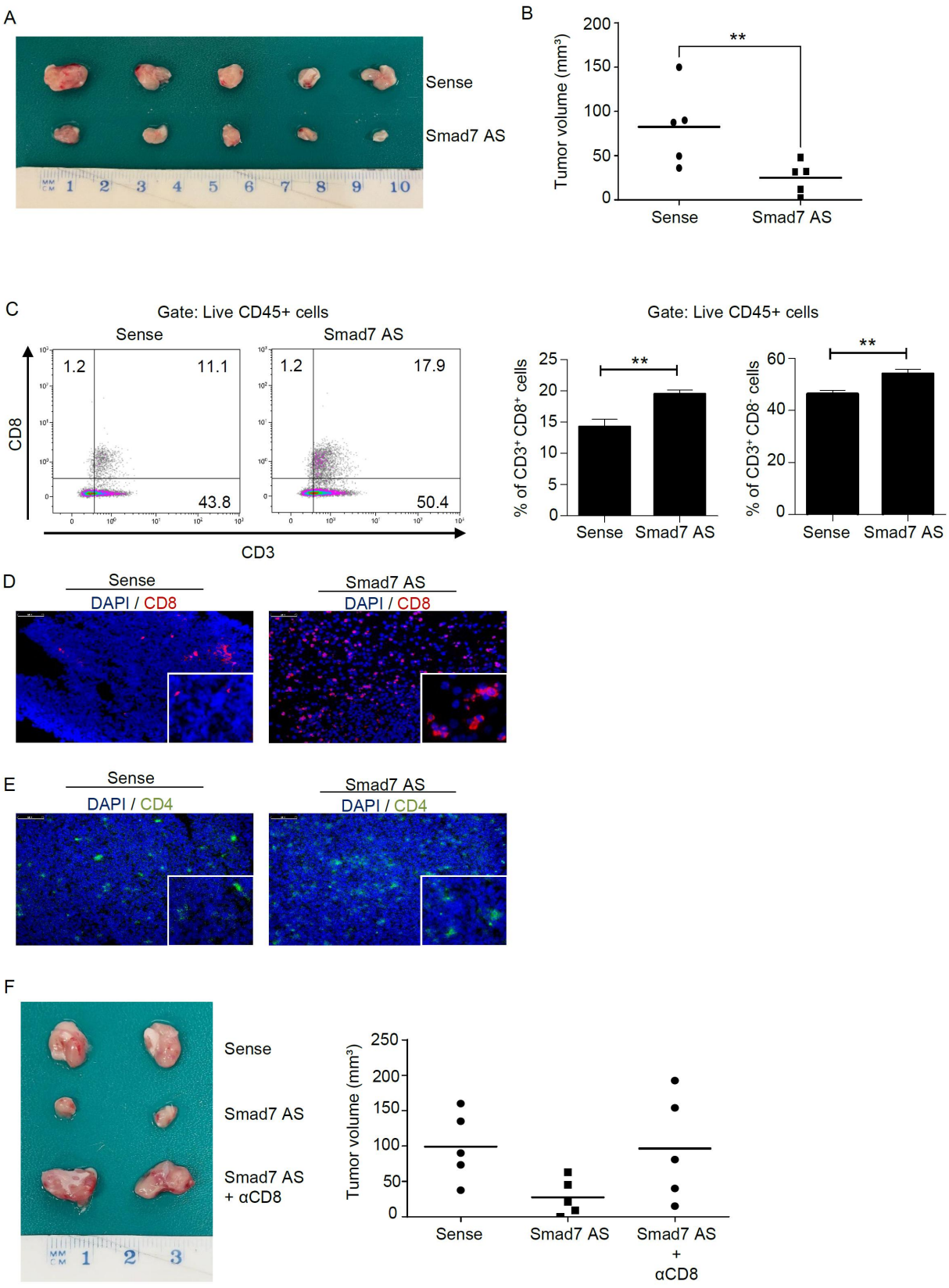


**Figure 4.** SMAD7-deficient CT26 cells engrafted in mice induce an anti-cancer $CD8^+$ T cell-dependent immune response. (A-B) Representative images and relative graphs showing the volume of CT26-derived tumors in BALB/c mice. CT26 cells were transfected with either Smad7 as or sense for 48 hours and subcutaneously injected into the left flank of mice (day 0). Tumor growth was monitored until sacrifice (day 14). Each point in the graph indicates the tumor volume in each mouse. $^{**}p < 0.01$. (C) Representative density plots and histograms (right panels) showing the frequency of $CD3^+CD8^+$ and $CD3^+CD8$- cells isolated from tumors taken from mice injected with CT26 cells as indicated in A. Data were analyzed using a two-tailed Student's t-test. $^{**}p < 0.01$. (D-E) immunofluorescence images of CD8 (red, D) or CD4 (green, E) expression in sections derived from tumors extracted from mice injected with CT26 cells as indicated in A. Nuclei are stained with 4′,6-diamidino-2-phenylindole (DAPI, blue). (F) Representative images and the relative graph (right panel) showing the volume of CT26-derived tumors. CT26 were transfected with either Smad7 as or sense for 48 hours and subcutaneously injected into the left flank of BALB/c mice (day 0). $CD8^+$ cell depletion was obtained upon intraperitoneal injections of anti-mouse CD8 antibody (every 4 days starting from day – 2 until day 10). Tumor growth was monitored until sacrifice (day 14). Each point in the graph represents the value of tumor volume in each mouse.

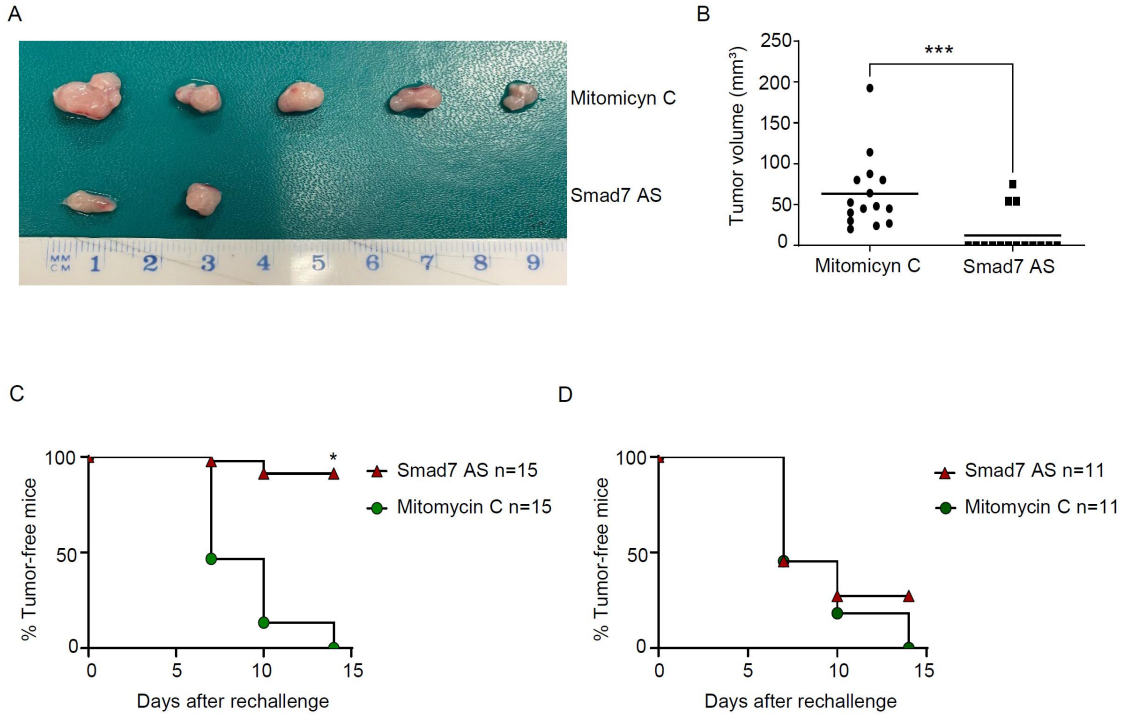


**Figure 5.** Smad7 protein downregulation induces immunogenic cell death. (A-B) Representative image and the relative graph (right panel) showing the volume of CT26-derived tumors in immunocompetent BALB/c mice vaccinated with mitomycin C-treated CT26 cells or Smad7 as transfected CT26 cells. Each point in the graph represents the tumor volume in each mouse. ***$p < 0.001$. (C-D) Percentage of tumor-free mice vaccinated with mitomycin C-treated CT26 cells or SMAD7 as transfected CT26 cells and challenged after 7 days with CT26 (C) or TS/A (D) cells. Tumor growth was monitored until sacrifice (day 14).

immunogenicity of tumor cells. For the in vitro studies we selected DLD1 and HCT-116 cells, as these cell lines express elevated levels of Smad7.[16] Antisense oligonucleotide-mediated inhibition of Smad7 protein expression was accompanied by enhanced exposure of CRT on the cell surface and increased secretion of HMGB1 and ATP. No significant increase in the percentage of ecto-CRT-expressing cells was seen following transfection with a non-relevant, cadherin-11 AS, thus excluding the possibility that the translocation of CRT on the surface of cells transfected with Smad7 AS was due to a nonspecific-effect of AS. We surmise that induction of ER stress in Smad7-deficient CRC cells is functionally relevant to the exposure of CRT on the cell surface because pre-treatment of cells with TUDCA, a chemical chaperone that inhibits ER stress,[25] prevented the Smad7 AS-mediated translocation of CRT on the CRC cell surface. Our findings are consistent with data from a previously published study documenting the ability of TUDCA to prevent doxorubicin-induced CRT cellular distribution in ovarian cancer cells.[6]

Co-cultures of CRC cells transfected with Smad7 sense or AS with human DCs showed that Smad7 deficiency increased DC activation as evidenced by the enhanced DC-mediated uptake of CRC cells and increased expression of HLA-DRII on DCs. Altogether these results raise the possibility that decreased Smad7 protein expression may directly mediate ICD in CRC cells. To further verify this hypothesis, we performed in vivo experiments and initially showed that mice engrafted with Smad7-deficient CT26 cells developed fewer and smaller tumors than animals engrafted with wild-type CT26 cells. Moreover, Smad7-deficient CT26-derived tumors contained more $CD8^+$ T cells and to a lesser extent $CD4^+$ T cells than wild-type CT26-derived tumors, and depletion of $CD8^+$ T cells abrogated the protective effect of Smad7 deficiency on the tumor development. Implanted Smad7-deficient CT26 cells protected mice from challenge with wild-type CT26. Notably, such protection by vaccination, the gold standard for ICD, was restricted to CRC cells as we were able to show no protection when mice were re-challenged with TS/A, a mammary cancer cell line that expresses a different repertoire of antigens.[23,26]

We are aware of the limitations of the present study. For instance, all the in vitro studies were performed using the same cancer cell lines (namely, DLD1, HCT-116, and CT26) in which we previously showed that reduction of Smad7 expression was accompanied by ER stress induction.[18] Therefore, these cell lines allowed us to further verify the link between Smad7 deficiency and induction of ER stress-driven ICD. We decided to inhibit Smad7 protein expression rather than using stable knockout cell lines because Smad7 is a positive regulator of CRC cell survival and stable Smad7-deficient cells would die rapidly in the cultures. For the in vivo studies, we used the mouse graft model. Although this model does not mimic the in vivo heterogeneity of human CRC, it was very useful in proving that the cell death induced by Smad7 deficiency is immunogenic, because the gold standard method to confirm the in vivo ICD induction is the vaccination rechallenge in mice engrafted with cancer cells.[23]

Altogether data of the present findings support the view that Smad7 plays a key role in sustaining CRC.[27] Single nucleotide polymorphisms (SNPs) in Smad7 gene have been documented in CRC patients and associated with an increased risk of such neoplasia as a result of their effect on Smad7 content in CRC cells.[28–30] Consistently, down-regulation of Smad7 in both

primary CRC cells and CRC cell lines alters the expression of molecules involved in the activation of pathways sustaining cancer cell growth and survival,[16,27] and functional studies showed that systemic administration of Smad7 inhibitors reduces the growth of CRC cell-derived grafts in mice.[16]

In conclusion, our results indicate that the reduction of Smad7 expression in CRC cells promotes cellular events that enhance antigenicity, activate cytotoxic T lymphocytes, and induce ICD. Further studies are, however, needed to validate the clinical significance of our findings and ascertain whether Smad7 inhibitors can be developed as novel ICD inducers, providing a new concept for antitumor immunotherapy.

## Acknowledgments

The authors wish to thank Nogra Pharma and PPM Services.

## Disclosure statement

G Monteleone served as a consultant for First Wave BioPharma, as a speaker for Takeda, AbbVie, Galapagos, and Pfizer, and filed a patent related to the treatment of inflammatory bowel diseases with Smad7 antisense oligonucleotides. The other authors declare no commercial or financial conflict of interest.

## Funding

This work was supported by PRIN HEAL ITALIA - PE6 (PE_00000019) (to G.M.) and by the Ministero dell´Università e della Ricerca (MUR), PRIN 2022, ID 2022JEBP88 (to C.S.) Ministero dell'Università e della Ricerca [PRIN HEAL ITALIA - PE6 (PE_00000019)]; Ministero dell'Università e della Ricerca [PRIN 2022, ID 2022JEBP88].

## ORCID

Carmine Stolfi http://orcid.org/0000-0002-6354-2443
Giovanni Monteleone http://orcid.org/0000-0003-1339-9076

## CRediT authorship contributions

C.M. Investigation, data curation, formal analysis, visualization; E.F., F.L. Investigation, formal analysis; M.C, A.I., R.F. investigation; I.M., conceptualization, resources; C.S. Visualization, supervision, validation, funding acquisition, writing – review & editing; G.M. Conceptualization, supervision, validation, funding acquisition, writing – review & editing. All authors confirm that they have reviewed and approved the journal's authorship agreement. All authors have read and agreed to the published version of the manuscript.

## Data availability statement

All datasets on which the conclusions of the paper rely is available to referees and to readers upon request.

## Ethics approval

All mouse experiments were approved by the local Institutional Animal Care and Use Committee (authorization 794/2023-PR), registered with the Italian Ministry of Health.

## References

1. Chong W, Zhu X, Ren H, Ye C, Xu K, Wang Z, Jia S, Shang L, Li L, Chen H. Integrated multi-omics characterization of KRAS mutant colorectal cancer. Theranostics. 2022;12(11):5138–5154. doi: 10.7150/thno.73089.
2. Zhao H, Ming T, Tang S, Ren S, Yang H, Liu M, Tao Q, Xu H. Wnt signaling in colorectal cancer: pathogenic role and therapeutic target. Mol Cancer. 2022;21(1):144. doi: 10.1186/s12943-022-01616-7.
3. Wu X, Yan H, Qiu M, Qu X, Wang J, Xu S, Zheng Y, Ge M, Yan L, Liang L. Comprehensive characterization of tumor microenvironment in colorectal cancer via molecular analysis. eLife. 2023;12:e86032. doi: 10.7554/eLife.86032.
4. Li F, Lin Y, Li R, Shen X, Xiang M, Xiong G, Zhang K, Xia T, Guo J, Miao Z, et al. Molecular targeted therapy for metastatic colorectal cancer: current and evolving approaches. Front Pharmacol. 2023;14:1165666. doi: 10.3389/fphar.2023.1165666.
5. Dudek AM, Garg AD, Krysko DV, De Ruysscher D, Agostinis P. Inducers of immunogenic cancer cell death. Cytokine & Growth Factor Rev. 2013;24(4):319–333. doi: 10.1016/j.cytogfr.2013.01.005.
6. Abdullah TM, Whatmore J, Bremer E, Slibinskas R, Michalak M, Eggleton P. Endoplasmic reticulum stress-induced release and binding of calreticulin from human ovarian cancer cells. Cancer Immunol Immunother CII. 2022;71(7):1655–1669. doi: 10.1007/s00262-021-03072-6.
7. Matsusaka K, Azuma Y, Kaga Y, Uchida S, Takebayashi Y, Tsuyama T, Tada S. Distinct roles in phagocytosis of the early and late increases of cell surface calreticulin induced by oxaliplatin. Biochem And Biophys Rep. 2022;29:101222. doi: 10.1016/j.bbrep.2022.101222.
8. Salvagno C, Cubillos-Ruiz JR. The impact of endoplasmic reticulum stress responses in dendritic cell immunobiology. In: International review of cell and molecular biology. Vol. 349. Elsevier; 2019. p. 153–176.
9. Garg AD, Dudek AM, Agostinis P. Cancer immunogenicity, danger signals, and DAMPs: what, when, and how? BioFactors. 2013;39(4):355–367. doi: 10.1002/biof.1125.
10. Vacchelli E, Ma Y, Baracco EE, Sistigu A, Enot DP, Pietrocola F, Yang H, Adjemian S, Chaba K, Semeraro M, et al. Chemotherapy-induced antitumor immunity requires formyl peptide receptor 1. Science. 2015;350(6263):972–978. doi: 10.1126/science.aad0779.
11. Li X, Zheng J, Chen S, Meng F, Ning J, Sun S. Oleandrin, a cardiac glycoside, induces immunogenic cell death via the PERK/elF2α/ATF4/CHOP pathway in breast cancer. Cell Death Dis. 2021;12(4):314. doi: 10.1038/s41419-021-03605-y.
12. De Silva M, Tse BCY, Diakos CI, Clarke S, Molloy MP. Immunogenic cell death in colorectal cancer: a review of mechanisms and clinical utility. Cancer Immunol Immunother CII. 2024;73(3):53. doi: 10.1007/s00262-024-03641-5.
13. Wang X, Ren L, Ye L, Cao J. Photodynamic therapy augments oxaliplatin-induced immunogenic cell death in colorectal cancer. Central Eur J Immunol. 2023;48(3):189–202. doi: 10.5114/ceji.2023.132053.
14. Jie Y, Yang X, Chen W. Pulsatilla decoction combined with 5-fluorouracil triggers immunogenic cell death in colorectal cancer cells. Cancer Biother Radiopharm. 2022;37(10):945–954. doi: 10.1089/cbr.2020.4369.
15. Chiaravalli M, Spring A, Agostini A, Piro G, Carbone C, Tortora G. Immunogenic cell death: an emerging target in gastrointestinal cancers. Cells. 2022;11(19):3033. doi: 10.3390/cells11193033.
16. Stolfi C, De Simone V, Colantoni A, Franzè E, Ribichini E, Fantini MC, Caruso R, Monteleone I, Sica GS, Sileri P, et al. A functional role for Smad7 in sustaining colon cancer cell growth and survival. Cell Death Dis. 2014;5(2):e1073–e1073. doi: 10.1038/cddis.2014.49.
17. Colella M, Iannucci A, Maresca C, Albano F, Mazzoccoli C, Laudisi F, Monteleone I, Monteleone G. SMAD7 sustains XIAP expression and migration of colorectal carcinoma cells. Cancers. 2024;16(13):2370. doi: 10.3390/cancers16132370.

18. De Simone V, Bevivino G, Sedda S, Izzo R, Laudisi F, Dinallo V, Franzè E, Colantoni A, Ortenzi A, Salvatori S, et al. Smad7 knockdown activates protein kinase RNA-associated eIf2α pathway leading to colon cancer cell death. Cell Death Dis. 2017;8(3):e2681–e2681. doi: 10.1038/cddis.2017.103.
19. Di Fusco D, Dinallo V, Marafini I, Figliuzzi MM, Romano B, Monteleone G. Antisense oligonucleotide: basic concepts and therapeutic application in inflammatory bowel disease. Front Pharmacol. 2019;10:305. doi: 10.3389/fphar.2019.00305.
20. Troncone E, Marafini I, Stolfi C, Monteleone G. Transforming growth factor-β1/Smad7 in intestinal immunity, inflammation, and cancer. Front Immunol. 2018;9:1407. doi: 10.3389/fimmu.2018.01407.
21. Maresca C, Di Maggio G, Stolfi C, Laudisi F, Colella M, Pacifico T, Di Grazia A, Di Fusco D, Congiu D, Guida AM, et al. Smad7 sustains Stat3 expression and signaling in colon cancer cells. Cancers. 2022;14(20):4993. doi: 10.3390/cancers14204993.
22. Gao W, Wang X, Zhou Y, Wang X, Yu Y. Autophagy, ferroptosis, pyroptosis, and necroptosis in tumor immunotherapy. Signal Transduct Targeted Ther. 2022;7(1):1–26. doi: 10.1038/s41392-022-01046-3.
23. Humeau J, Lévesque S, Kroemer G, Pol JG. Gold standard assessment of immunogenic cell death in oncological mouse models. In: López-Soto A Folgueras A. editors. Cancer immunosurveillance. Vol. 1884. New York (NY): Springer New York; 2019. p. 297–315. Methods in Molecular Biology.
24. Troncone E, Monteleone G. Smad7 and colorectal carcinogenesis: a double-edged sword. Cancers. 2019;11(5):612. doi: 10.3390/cancers11050612.
25. Laudisi F, Di Fusco D, Dinallo V, Stolfi C, Di Grazia A, Marafini I, Colantoni A, Ortenzi A, Alteri C, Guerrieri F, et al. The food additive maltodextrin promotes endoplasmic reticulum stress–driven mucus depletion and exacerbates intestinal inflammation. Cellular Mol Gastroenterol Hepatol. 2019;7(2):457–473. doi: 10.1016/j.jcmgh.2018.09.002.
26. Stringhini M, Probst P, Neri D. Immunotherapy of CT26 murine tumors is characterized by an oligoclonal response of tissue-resident memory T cells against the AH1 rejection antigen. Eur J Immunol. 2020;50(10):1591–1597. doi: 10.1002/eji.201948433.
27. Stolfi C, Marafini I, De Simone V, Pallone F, Monteleone G. The dual role of Smad7 in the control of cancer growth and metastasis. Int J Mol Sci. 2013;14(12):23774–23790. doi: 10.3390/ijms141223774.
28. Wu Y, Xu J, Tan B, Yi T, Liu S, Yang G, Li K, Zhao X. SMAD7 gene polymorphisms and their influence on patients with colorectal cancer. Cell Cycle. 2023;22(21–22):2424–2435. doi: 10.1080/15384101.2023.2296210.
29. Liu Z, Zhao Y, Song H, Miao H, Wang Y, Tu C, Fu T, Qin J, Du B, Qian M, et al. Identification and characterization of colorectal-cancer-associated SNPs on the SMAD7 locus. J Cancer Res Clin Oncol. 2023;149(18):16659–16668. doi: 10.1007/s00432-023-05402-w.
30. Rosic J, Miladinov M, Dragicevic S, Eric K, Bogdanovic A, Krivokapic Z, Nikolic A. Genetic analysis and allele-specific expression of SMAD7 3′UTR variants in human colorectal cancer reveal a novel somatic variant exhibiting allelic imbalance. Gene. 2023;859:147217. doi: 10.1016/j.gene.2023.147217.